MICROCOPY RESOLUTION TEST CHART
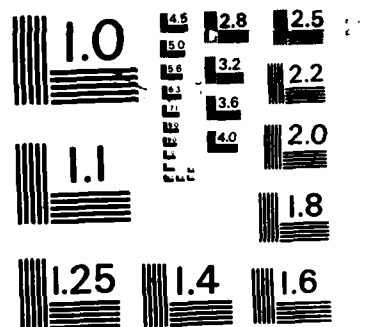
NATIONAL BUREAU OF STANDARDS-1963-A

RADC-TR-83-285
In-House Report
December 1983

STATIC FREQUENCY-TEMPERATURE CHARACTERISTICS OF DOUBLY ROTATED QUARTZ

Alfred Kahan

APPROVED FOR PUBLIC RELEASE; DISTRIBUTION UNLIMITED

AD-A142 456

DTIC FILE COPY

ROME AIR DEVELOPMENT CENTER
Air Force Systems Command
Griffiss Air Force Base, NY 13441

84 06   003

REPORT DOCUMENTATION PAGE	READ INSTRUCTIONS BEFORE COMPLETING FORM

1 REPORT NUMBER	2 GOVT ACCESSION NO	3 RECIPIENT'S CATALOG NUMBER
RADC-TR-83-285	AI42456	

4 TITLE (and Subtitle)	5 TYPE OF REPORT & PERIOD COVERED
STATIC FREQUENCY-TEMPERATURE CHAR- ACTERISTICS OF DOUBLY ROTATED QUARTZ	In-house report July 82 - August 83
	6 PERFORMING ORG REPORT NUMBER

7 AUTHOR(s)	8 CONTRACT OR GRANT NUMBER(s)
Alfred Kahan	

9 PERFORMING ORGANIZATION NAME AND ADDRESS	10 PROGRAM ELEMENT PROJECT TASK AREA & WORK UNIT NUMBERS
Solid State Sciences Division (RADC/ES) Rome Air Development Center Hanscom AFB MA 01731	PE61102F 2305J104

11 CONTROLLING OFFICE NAME AND ADDRESS	12 REPORT DATE
Solid State Sciences Division (RADC/ES) Rome Air Development Center Hanscom AFB MA 01731	December 1983
	13 NUMBER OF PAGES
	40

14 MONITORING AGENCY NAME & ADDRESS(if different from Controlling Office)	15 SECURITY CLASS (of this report)
	Unclassified
	15a DECLASSIFICATION DOWNGRADING SCHEDULE

16 DISTRIBUTION STATEMENT (of this Report)

Approved for public release; distribution unlimited.

17 DISTRIBUTION STATEMENT (of the abstract entered in Block 20, if different from Report)

18 SUPPLEMENTARY NOTES

19 KEY WORDS (Continue on reverse side if necessary and identify by block number)

Quartz
Crystal resonators
Frequency standards

20 ABSTRACT (Continue on reverse side if necessary and identify by block number)

The static frequency characteristics of crystallographically doubly rotated quartz as a function of temperature, f(T), are described. Curves showing the sensitivity of the normalized frequency offset to small misorientations in angle are developed. Three different sets of currently accepted temperature coefficients of elastic constants are applied to calculate f(T). We show that for specific orientations of practical interest, the three sets predict significant differences in the inflection and turnover temperatures. The crystallographic orientations showing this angular sensitivity are the ones to be exploited

DD FORM 1473 EDITION OF 1 NOV 65 IS OBSOLETE
1 JAN 73

20. Abstract - Contd.

experimentally to establish the regions in which the different sets are valid. Detailed computations are performed for orientations yielding 80° C turnover temperatures and for the SC-cut.

Preface

The author is indebted to Virgil Vickers for providing versatile graphic
display and plotting programs. Appreciation is also expressed to Ferdinand Euler
for his scrutiny of the manuscript and many valuable comments.

3

Contents

Illustrations

7

Static Frequency-Temperature
Characteristics of Doubly Rotated Quartz

I. INTRODUCTION

Single crystal α-quartz is the most commonly used material for piezoelec-
tric resonators. It is chosen because of its superior mechanical, physical, and
chemical properties. The most important performance parameter of a crystal
resonator is the static temperature-dependent frequency characteristic, f(T), of
the device. The temperature dependence of the frequency is determined by the
elastic, piezoelectric, and dielectric constants of the resonating crystal, their
temperature dependencies, and the crystal expansion coefficients. In the tem-
perature range from -200 to +200 °C, f(T) of the thickness mode vibrations of
quartz is described well by a third order polynomial.[1] Explicit algebraic equa-
tions relating the three coefficients of the polynomial to the material constants
and their temperature coefficients are summarized in References 2 and 3.
Quartz belongs to the trigonal crystal system, and material properties are
crystal-orientation dependent. Orientations exist that give relatively flat f(T)

1. Bechmann, R., Ballato, A.D., and Lukaszek, T.J. (1962) Higher-order
   temperature coefficients of elastic stiffnesses and compliances of α-quartz,
   Proc. IRE 50:1812-1822.

2. Kahan, A. (1982) Elastic Constants of Quartz, RADC-TR-82-117, AD A121672.

3. Kahan, A. (1982) Temperature Coefficients of the Elastic Constants of Quartz,
   RADC-TR-82-224, AD A125709.

over a wide temperature range. Typical examples include the singly rotated AT- and BT-cuts, and the doubly rotated SC-cut.

The frequency may exhibit extremes as a function of temperature. The temperatures corresponding to the frequency maximum and minimum are designated as the turnover temperatures, T_{to}. For high stability oscillator applications, the resonator is enclosed in a precisely controlled oven and maintained at one of the T_{to} points. Most military applications specify maximum temperatures to which the oscillator may be exposed to be between 60 and 100 ^{o}C. The crystal orientation is then selected to generate one T_{to} several degrees above this upper environmental temperature. Because T_{to} is sensitive to crystallographic orientation, the tolerances on cutting the crystal are narrow, of the order of minutes or seconds of arc, and these tolerances must be maintained throughout the resonator fabrication process. Both requirements, precise oven control and accurate crystal orientation, affect the oscillator costs considerably.

The singly rotated AT- and BT-cuts are the crystal orientations most widely used for high-stability applications. In the temperature range of practical interest, the doubly rotated cuts, for example, the SC-cut, can have considerably smaller frequency variation.[4] In principle, one can obtain several orders of magnitude decrease in temperature sensitivity, but, in practice, this decrease is coupled with considerably narrower angular tolerances. Doubly rotated orientations of interest include, in addition to the SC-cut, the IT-, FC-, RT-, and LC-cuts. This topic has been reviewed extensively by Ballato.[5]

There are several ways to define the temperature-insensitive orientations. The most common one, exemplified by Ballato,[5] is the angular orientation corresponding to zero values of the first order coefficient of temperature: $a_o = 0$. Cuts situated along $a_o = 0$ angles are attractive because only the second and third order coefficients b_o and c_o contribute to the frequency offset, and f(T) becomes a slowly varying function of temperature. Resonator parameters of interest include the positions of the inflection and turnover temperatures, T_i and T_{to}, and the magnitude of frequency variation around T_{to}. These parameters are determined by all three coefficients and are not necessarily optimized at the angles corresponding to $a_o = 0$. Another description references the angular positions of the temperature-insensitive cuts to the orientations determined by $T_i = T_{to}$.

4. Kusters, J.A., Adams, C.A., Yashida, H., and Leach, J.G. (1977) TTC's - Further developmental results, 31st Annual Symposium on Frequency Control, 3-7.

5. Ballato, A.D. (1977) Doubly rotated thickness mode plate vibrators, Physical Acoustics, Vol. XIII, W.P. Mason and T.N. Thurston, Eds., Academic Press, New York, pp. 115-181.

There are three sets of temperature coefficients of elastic constants $T_n(c_{pq})$ that can be applied equally well for calculating f(T). In Reference 3, these sets are designated as BBL(1962), BBL(1963), and Adams et al. All f(T) calculations reported in the literature are based on BBL(1962). In References 2 and 3 it was shown that BBL(1962) may not predict the f(T) characteristics of arbitrary doubly rotated orientations well, and instead, BBL(1963) LSF were chosen as the working set of material constants. In this report, the three $T_n(c_{pq})$ sets are applied to illustrate f(T), and show that for specific doubly rotated orientations, the three sets predict significant angular differences in the positions of $T_i = T_{to}$ or $a_o = 0$. These crystallographic orientations showing this angular sensitivity can be exploited to determine $T_n(c_{pq})$.

2. COORDINATE SYSTEM

Figure 1 depicts the Y-cut plate geometry and crystallographic coordinate system used in this investigation. The initial position of the plate is aligned with the x-, y-, and z-axes. The position of the rotated plate, x', y, and z', is described by angles (ϕ, θ), where ϕ and θ are rotations around the z- and x-axes, respectively. Owing to crystal symmetries applicable to quartz, all rotations are mapped into

$$0 \leq \phi \leq 60^{\circ} \quad \text{and} \quad 0 \leq \theta \leq 90^{\circ} \quad .$$

In this nomenclature, the approximate values of φ and θ for the AT-, BT-, and SC-cuts are $(0, 35)^{\circ}$, $(60, 49)^{\circ}$, and $(22, 34)^{\circ}$, respectively. Another commonly used mapping region is

$$0 \leq \phi' \leq 30^{\circ} \quad \text{and} \quad -90 \leq \theta' \leq +90^{\circ} \quad .$$

For $\phi > 30^{\circ}$, the two descriptions are related by the transformation

$$\phi' = 60^{\circ} - \phi \quad \text{and} \quad \theta' = -\theta \quad .$$

In the (ϕ', θ') nomenclature, the BT-cut becomes $(0, -49)^{\circ}$, and, for example, the combination $(40^{\circ}54', 16^{\circ}34')$ transforms to $(19^{\circ}06', -16^{\circ}34')$.

11
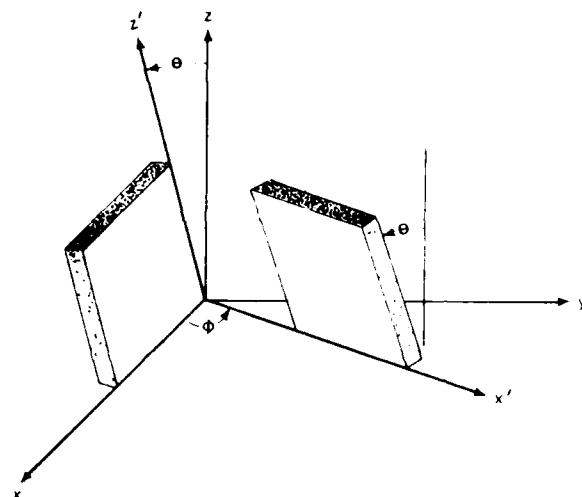
Figure 1. Coordinate System for a Doubly
Rotated Crystal Plate

3. TEMPERATURE DEPENDENCE OF FREQUENCY

In a series of experiments, Bechmann, Ballato, and Lukaszek[1, 6] have
evaluated the frequency as a function of static temperature characteristics of
quartz resonators in the temperature range of -200 to +200 $^{\circ}$C. They have
shown that the normalized frequency offsets of the transverse mode vibrations
are described well by a cubic equation of the form

$$f(T) \equiv f(T, \phi, \theta) = \frac{\Delta f}{f_o} = \frac{f - f_o}{f_o} = \sum_{n=1}^{3} f_n(\phi, \theta)(T - T_o)^n$$

$$= a_o(T - T_o) + b_o(T - T_o)^2 + c_o(T - T_o)^3 \quad ,$$

(1)

where f is the frequency at temperature T, f_o the frequency at the reference
temperature T_o, and $f_n(\phi, \theta)$ are the first, second, and third order temperature
coefficients evaluated at T_o. In most applications the series is expanded using

---

6. Bechmann, R., Ballato, A.D., and Lukaszek, T.J. (1963) Higher-Order
     Temperature Coefficients of Elastic Stiffnesses and Compliances of
     α-Quartz, USAELRDL TR 2261.

12

the reference temperature $T_o = 25\ {}^\circ C$. For ease of notation we designate $f_1(\phi, \theta)$, $f_2(\phi, \theta)$, and $f_3(\phi, \theta)$ as a_o, b_o, and c_o, respectively.

For quartz, $f_n(\phi, \theta)$ are calculated from the six elastic, two dielectric, and two piezoelectric constants, the temperature dependencies of these constants, and the two expansion coefficients of the material. In References 2 and 3 we discuss the validity of currently accepted material constant values of quartz, and we list three alternate sets of $T_n(c_{pq})$. The first, designated as BBL(1962), is the one listed in Bechmann, Ballato, and Lukaszek,[1] and is derived from data reported in that publication. The second set, designated as BBL(1963) LSF, is derived in Reference 3, and is based on the least squares fit of the data published by Bechmann, Ballato, and Lukaszek.[6] The third set, designated as Adams et al, is given by Adams, Enslow, Kusters, and Ward.[7] Unless noted otherwise, the numerical results of this report are based on BBL(1963) LSF. For illustration purposes, the particular $T_n(c_{pq})$ set used to calculate T_i, T_{to}, or $f(T)$ is not critical. All sets give similar results, and no conclusions can be drawn regarding the superiority of a particular set. However, the three $T_n(c_{pq})$ sets do show substantial numerical differences in predicting $f(T)$ characteristics for specific (ϕ, θ) orientations, for example, the SC-cut. There is now extensive experimental data available on the SC-cut, and, in turn, this data can be utilized to rederive $T_n(c_{pq})$ values.

4. MATHEMATICAL PROPERTIES OF CUBIC CURVES

Bechmann[6,8] described the mathematical properties of Eq. (1), which gives the variation of the vibration frequency of a quartz plate as a function of temperature.

By definition, all $\Delta f/f_o$ as a function of T curves have a root at T_o. In addition, two additional roots, $T_{r,s}$ are at

$$T_{r,s} = T_o - \frac{1}{2c_o}\left[b_o \pm (b_o^2 - 4a_o c_o)^{1/2}\right] \ . \tag{2}$$

7. Adams, C.A., Enslow, G.M., Kusters, J.A., and Ward, R.W. (1970) Selected topics in quartz crystal research, 24th Annual Symposium on Frequency Control, 55-63, AD 746210.

8. Bechmann, R. (1956) Frequency-temperature-angle characteristics of AT-type resonators made of natural and synthetic quartz, Proc. IRE 44:1600-1607.

The temperature positions of the maxima in $f(T)$, designated as the turnover temperatures T_{to}, are symmetric around the inflection temperature T_i, and are obtained by differentiating Eq. (1),

$$T_{to} = \left(T_o - \frac{b_o}{3c_o}\right) \pm \frac{1}{3c_o}(b_o^2 - 3a_o c_o)^{1/2}$$

$$= T_i \pm \left[(T_i - T_o)^2 - a_o/3c_o\right]^{1/2} \quad , \tag{2}$$

where

$$T_i = T_o - \frac{b_o}{3c_o} \quad . \tag{3}$$

All $f(T)$ curves have an inflection temperature, but the existence of T_{to} and three real roots depends whether the radical terms in Eqs. (2) and (3) are real or imaginary. The existence of three roots automatically implies the existence of T_{to}, but the existence of T_{to} does not necessarily insure that $\Delta f/f_o = 0$ is satisfied at three points.

The general behavior of $f(T)$ based on BBL(1963) LSF is illustrated in Figures 2 and 3 for c-mode AT-cut ($\phi = 0°$) and b-mode BT-cut ($\varphi = 60°$) quartz plates, respectively. In the -60 to +100 °C range, the slopes of the AT-cut curves decrease with increasing n-values; at $(0, 35.25)°$ the radical term of Eq. (3) vanishes and $T_{to} = T_i = 11.86$ °C. For $(0, 35.5)°$, T_i increases to $T_i = 16.75$ °C, the T_{to} are at -47.00 and 80.51 °C, and the roots are at -97.57, 25, and 122.82 °C, respectively. Similar considerations apply to the BT-cut. At $(60, 50.81)°$ the radical term of Eq. (3) vanishes and $T_{to} = T_i = -96.30$ °C.

The normalized frequency offset at T_i is

$$\left(\frac{\Delta f}{f_o}\right)_i = \left(b_o/27c_o^2\right)\left(2b_o^2 - 9a_o c_o\right) \tag{5}$$

and at T_{to}

$$\left(\frac{\Delta f}{f_o}\right)_{to} = \left(1/27c_o^2\right)\left[\left(2b_o^3 - 9a_o b_o c_o\right) \mp 2\left(b_o^2 - 3a_o c_o\right)^{3/2}\right]$$

$$= \left(\frac{\Delta f}{f_o}\right)_i - 2c_o(T_{to} - T_i)^3 \quad . \tag{6}$$

14
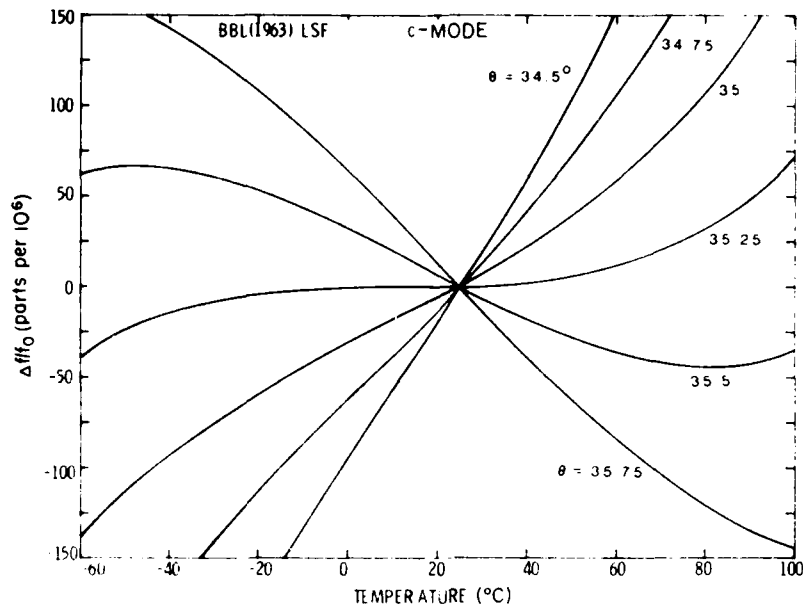
Figure 2. Normalized Frequency Offset as a Function of Temperature and θ-angle Orientation for the AT-cut, $\varphi = 0°$
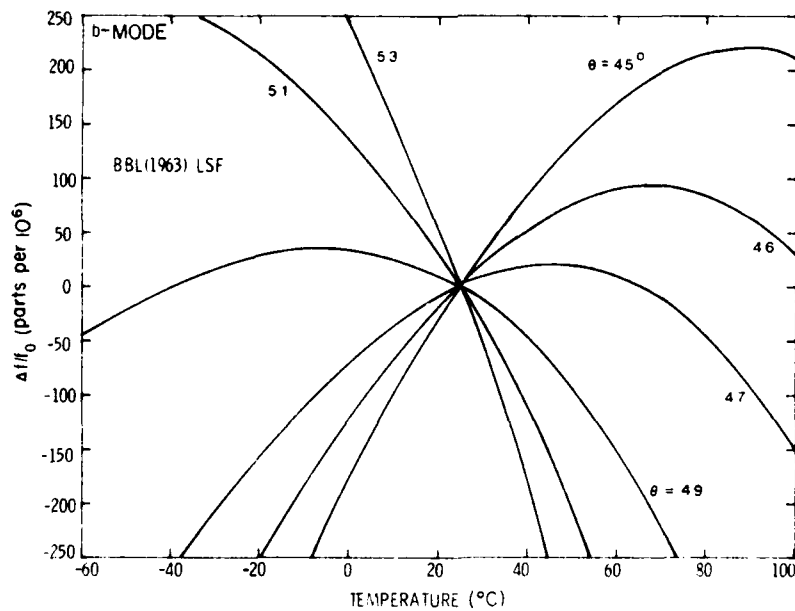
Figure 3. Normalized Frequency Offset as a Function of Temperature and θ-angle Orientation for the BT-cut, $\phi = 60°$

15

At T_{to}, the normalized frequency offsets are slowly varying functions of temperature, and, in a controlled environment, one is able to obtain high stability operations. Figures 4 and 5 show $\Delta f/f_o$ for T_{to} near 80 °C for the AT- and BT-cuts, respectively. At T_{to}, the temperature dependence of frequency for the AT-cut is $20 \times 10^{-9}/°C$ and for the BT-cut it is $60 \times 10^{-9}/°C$. These figures also show the sensitivity of $\Delta f/f_o$ to small changes in θ. Shifts occur both in the T_{to} positions and in $\Delta f/f_o$. In fabricating resonators, the f_o translation due to θ-angle misorientation is compensated by adjusting the plate thickness, and the major practical effect of misorientation is a shift in T_{to}. For T_{to} between 50 and 100 °C, the T_{to} shifts by 2.6 °C/minute of arc for the AT-cut, and 0.35 °C/minute of arc for the BT-cut.
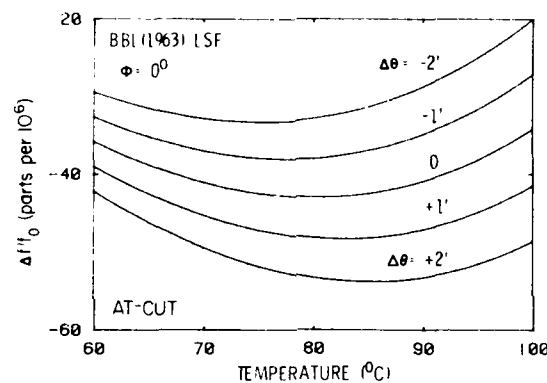
Figure 4. Sensitivity of Normalized Frequency Offset to Small θ-angle Variation for the AT-cut Around 80 °C Turnover Temperature

In many experiments, f(T) data is unavailable at T_o = 25 °C, and the normalized frequency is fitted with a cubic equation

$$\Delta f/f_1 = a_1(T - T_1) + b_1(T - T_1)^2 + c_1(T - T_1)^3 \tag{7}$$

referenced to temperature T_1 with coefficients a_1, b_1, and c_1. The transformation to reference temperature T_o is given by

$$a_o = \left[a_1 + 2b_1(T_o - T_1) + 3c_1(T_o - T_1)^2 \right]/p \tag{8}$$

16
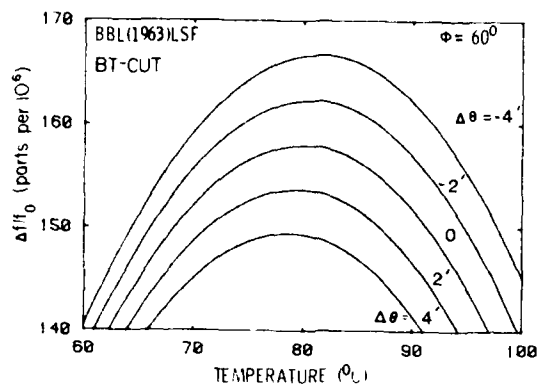
Figure 5. Sensitivity of Normalized Frequency Offset to Small θ-angle Variation for the BT-cut Around 80 $^\circ$C Turnover Temperature

$$b_o = [b_1 + 3c_1(T_o - T_1)]/p \qquad (9)$$

$$c_o = c_1/p \qquad (10)$$

$$p = 1 + a_1(T_o - T_1) + b_1(T_o - T_1)^2 + c_1(T_o - T_1)^3 \quad . \qquad (11)$$

Of particular interest is the normalized frequency offset referenced to T_i. This function, anti-symmetric with respect to T_i, is given by

$$(f - f_i)/f_i = [a_i + c_i(T - T_i)^2](T - T_i) \quad , \qquad (12)$$

where

$$a_i = -\left(b_o^2 - 3a_o c_o\right)/3c_o q \qquad (13)$$

$$c_i = c_o/q \qquad (14)$$

and

17

$$q = \frac{f_i}{f_o} = 1 + \frac{b_o\left(2b_o^2 - 9a_o c_o\right)}{27 c_o^2} \quad . \tag{15}$$

The turnover temperatures, symmetric with respect to T_i, are given by

$$T_{to} = T_i \pm \left(\frac{-a_i}{3c_i}\right)^{1/2} \quad . \tag{16}$$

5. ANGULAR ROTATIONS FOR $a_o = 0$ AND $T_i = T_{to}$

Ballato[5] illustrates many $f(T)$ characteristics of doubly rotated crystal cuts by considering the loci of the angular orientations (ϕ, θ) corresponding to the special case of $a_o = 0$. In this report, we prefer to reference characteristics to the condition of the two turnover temperatures coalescing with the inflection temperature, $T_i = T_{to}$. The corresponding angles are also known as the "zero-angles", or the "ideal" angles, and $f(T)$ variations around $T_i = T_{to}$ remain small over a wide temperature range.[9] Mathematically this condition is satisfied when $b_o^2 - 3a_o c_o = 0$. Figure 6 illustrates the difference between the two formulations for the c-mode at $\phi = 0^\circ$. The $T_i = T_{to}$ curve is the one depicted in Figure 2, $\theta = 35.249^\circ$, and it corresponds to the lower limit of θ-angles with real maxima. The θ-angle for $a_o = 0$ is $\theta = 35.259^\circ$. The 0.6 minute of arc difference between the two θ-angles is sufficient to cause parts per million offsets in $f(T)$.

An inspection of Eq. (3) shows that for $a_o = 0$ the T_{to} are real, and that they are located at T_o and at $2T_i - T_o$. The special case of $a_o = 0$ describes the condition of one T_{to} restricted to T_o. For the $a_o = 0$ curve shown in Figure 6, $T_i = 12.07\ ^\circ C$, $T_{to} = -0.87$ and $25\ ^\circ C$, whereas the temperature corresponding to the "zero-angle" is $T_i = T_{to} = 11.86\ ^\circ C$. Figure 7 shows the c-mode (ϕ, θ) loci for $a_o = 0$, between $\phi = 0^\circ$ and $\phi = 30^\circ$ based on BBL(1962) and BBL(1963) LSF. The figure also includes a graphic representation of the straight line formula for $a_o = 0$ given by Ballato in Reference 5, Eq. (85). We note that at $\phi = 22^\circ$, near the SC-cut, the θ-angle based on BBL(1963) LSF is 34.50°, the θ-angle based on BBL(1962) is 34.00°, and the straight line approximation gives 33.91°. The corresponding θ-angle computed from Adams et al is 33.86°. At higher ϕ-angles the divergence increases, and, for example, at $\varphi = 30^\circ$ the difference in θ based on the two $T_n(c_{pq})$ sets is more than 1°. Considering the fact

9. Vig, J., Washington, J.W., and Filler, R.L. (1981) Adjusting the frequency vs. temperature characteristics of SC-cut resonators by contouring, 35th Annual Symposium on Frequency Control, 104-109.

18
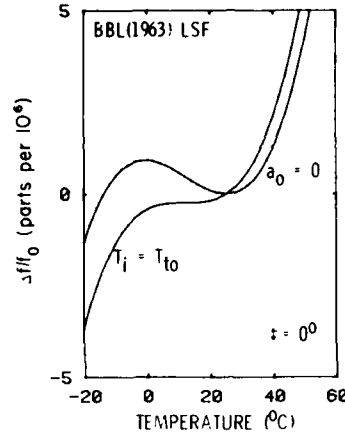
Figure 6. Comparison of Normalized Frequency Offsets as a Function of Temperature for $\phi = 0^O$ Oriented for "Zero-Angle" ($T_i = T_{to}$), and for Zero First Order Temperature Coefficient ($a_o = 0$)

that for any ϕ, $a_o = 0$ rigorously defines $T_{to} = 25^OC$, the substantial differences in θ-angles predicted by the $T_n(c_{pq})$ sets are easily accessible to experimental verifications.

Figure 8 shows the c-mode (ϕ, θ) loci for $T_i = T_{to}$ based Adams et al, BBL(1962), and BBL(1963) LSF parameters, respectively. At higher ϕ-angles, similar to $a_o = 0$, the curves diverge. Figure 9 shows the corresponding $T_i = T_{to}$. For all cases, $T_i = T_{to}$ increase with ϕ, but there are substantial differences in numerical values. Figures 10 and 11 show the first, second, and third order temperature coefficients a_o, b_o, and c_o, for $T_i = T_{to}$ based on the BBL(1963) LSF parameters. At $\phi = 10.56^O$, $a_o = b_o = 0$, and $T_i = T_{to} = T_o = 25\ ^OC$.

Figure 12 shows c-mode $(f - f_i)/f_i$ as a function of temperature for $T_i = T_{to}$ and several ϕ-angles normalized to their respective frequencies at $T_i = T_{to}$. Consistent with the fact that T_i increases with ϕ, the "flat" region of the curve shifts to higher temperature, and at the same time it becomes broader. This can be seen in a clearer manner by noting that in Eqs. (12) - (15), for $T_i = T_{to}$, $a_i = 0$, $q = 1 - (a_o b_o / 9c_o) \approx 1$, and the normalized frequency offset referenced to T_i reduces to

19
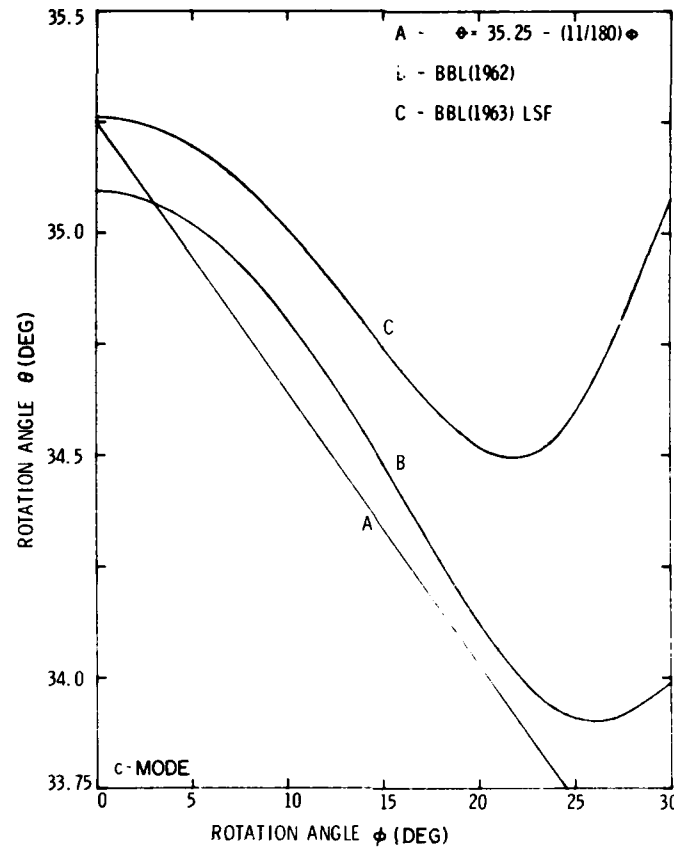
Figure 7. Loci in ϕ and θ of Zero First Order Temperature Coefficients of Frequency, $a_o = 0$, Based on BBL(1962) and BBL(1963) LSF Determined Temperature Coefficients of Elastic Constants

$$\frac{(f - f_i)}{f_i} \approx c_o(T - T_i)^3 \quad . \tag{17}$$

Figure 11 showed that c_o decreases with increasing ϕ. Thus, for the same temperature difference, $(f - f_i)/f_i$, proportional to c_o, will also decrease with increasing ϕ.

The frequency offset ΔF_i, for a temperature range $\Delta T = \pm(T - T_i)$ around $T_i = T_{to}$, is

$$\Delta F_i = c_i(T - T_i)^3 = 2c_i(\Delta T)^3 = 2(c_o/q)(\Delta T)^3 \approx 2c_o(\Delta T)^3 \quad . \tag{18}$$

20
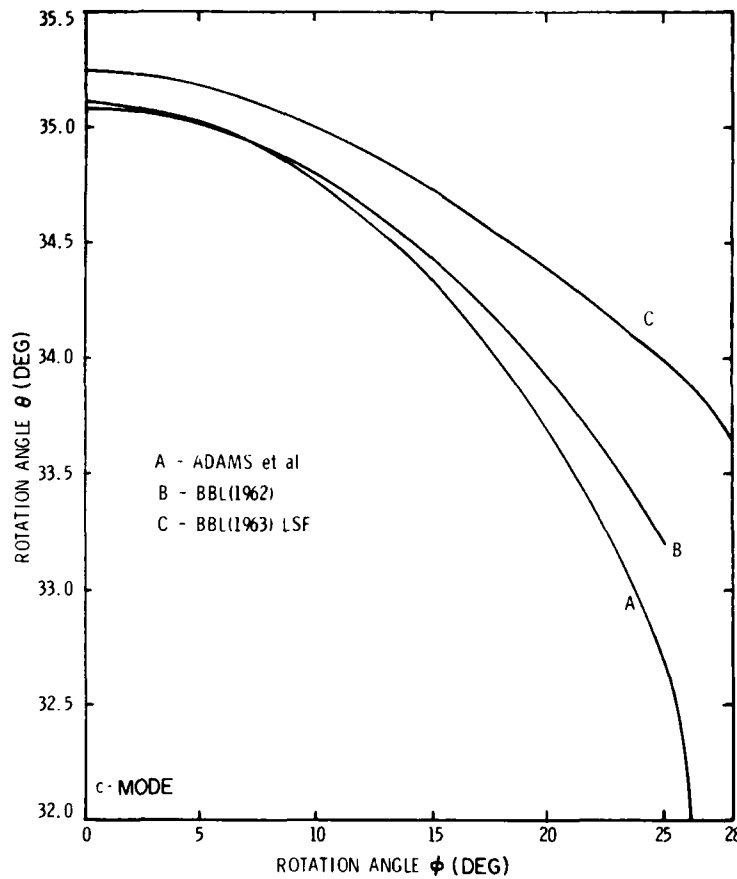
Figure 8. Loci in ϕ and θ of $T_i = T_{to}$ Based on Three Different Sets of Temperature Coefficients of Elastic Constants

Figure 13 shows ΔF_i between 79 and 81 $^\circ$C for $T_i = T_{to} = 80$ $^\circ$C. For $\Delta T = T - T_i = \pm 1$ $^\circ$C, $\Delta F_i = 11.2 \times 10^{-11}$. The f(T) curve corresponding to $T_i = T_{to}$ does not define the absolute frequency minimum between two temperatures. It is generally true (Reference 6) that for any temperature range $\pm \Delta T$, depicted in the top scale of Figure 13, the minimum frequency offset is obtained by choosing (ϕ, θ) so that T_i is halfway between $-\Delta T$ and $+\Delta T$ and T_{to} are situated at $\pm \Delta T/2$. The frequency offset for the minimum condition [Eq. (6)] is given by

$$\Delta F_{min} = -2 c_o \left(\frac{-\Delta T}{2} \right)^3 + 2 c_o \left(\frac{\Delta T}{2} \right)^3 = \frac{c_o}{2} (\Delta T)^3 \tag{19}$$

and the $(f - f_i)/f_i$ values are equal at $-\Delta T$ and $\Delta T/2$ (the upper T_{to}), and at $+\Delta T$ and $-\Delta T/2$ (the lower T_{to}). Figure 13 also shows f(T) corresponding to ΔF_{min},

21
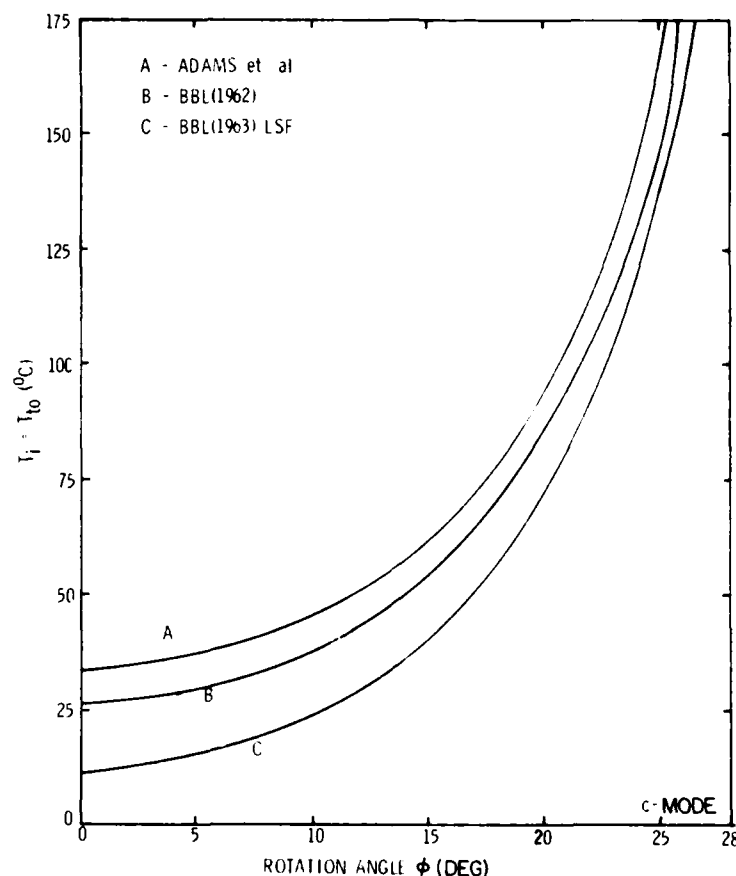
Figure 9.   Loci of $T_i = T_{to}$ as a Function of Rotation Angle ϕ

which satisfies $T_i = 80\ ^{\circ}C$ and $T_{to} = 79.5$ and $80.5\ ^{\circ}C$, respectively.   The normalized frequency offsets are equal at 79 and $80.5\ ^{\circ}C$, and at 79.5 and 81 $^{\circ}C$, and $\Delta F_{min} = 2.84 \times 10^{-11}$. $T_i = T_{to} = 80\ ^{\circ}C$ uniquely defines ϕ as $\phi = 20.71^{\circ}$, whereas T_{to} determines θ.   The difference in the ΔF_i and ΔF_{min} θ-angles is very small, $\Delta\theta = 0.047''$, but this is sufficient to reduce the frequency offsets by a factor of 4.   The c_o values corresponding to the two curves of Figure 13 are nearly identical.   Equations (18) and (19) show that for $\pm\Delta T$ both ΔF_i and ΔF_{min} increase as $(\Delta T)^3$ and that $\Delta F_i/\Delta F_{min} \approx 4$.   For example for $\Delta T = \pm 10$, that is, for the temperature range from 70 to 90 $^{\circ}C$, the frequency offset corresponding to $T_i = T_{to}$ is $\Delta F_i = 1.12 \times 10^{-7}$, a factor of 10^3 larger than for $\Delta T = \pm 1$, whereas the minimum frequency is obtained by choosing the θ-angle such as to position T_{to} at 75 and 85 $^{\circ}C$.   This gives $\Delta F_{min} = 2.84 \times 10^{-8}$, a factor of 10^3 larger than for $\Delta T = \pm 1$, but a factor of 4 smaller than ΔF_i.

22
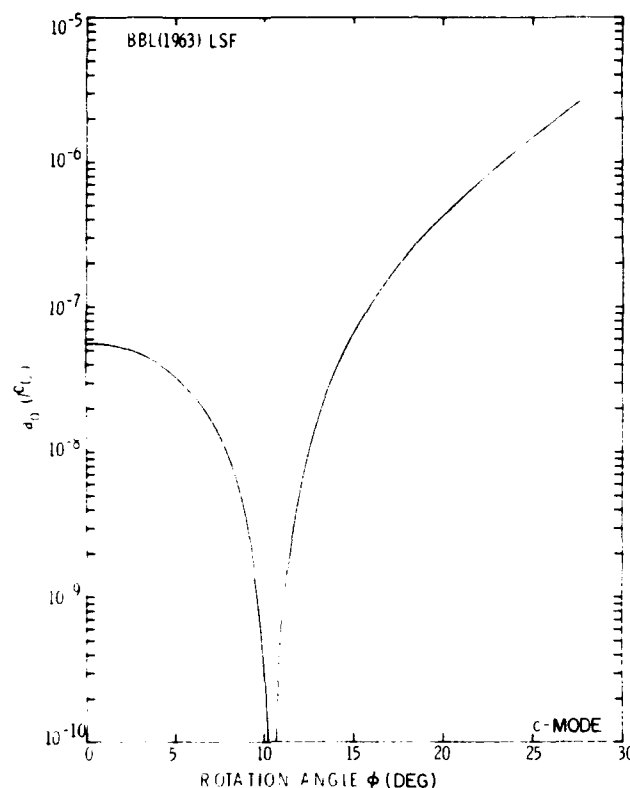
Figure 10. First Order Temperature Coefficients
of Frequency of the c-mode at $T_i = T_{to}$ as a Func-
tion of Rotation Angle ϕ

Consequently, the "zero-angle" is not the "ideal" angle to get a minimum vari-
ation of the static f(T).

The following example illustrates the recipe for selecting the optimum
doubly rotated (ϕ, θ) orientation for the minimum frequency offset, ΔF_{min}, in
any temperature range $\pm\Delta T$. Assume that the temperature range of interest
extends from -55 to +85 $^\circ$C. This defines $\Delta T = \pm 70$ $^\circ$C, $T_i = 15$ $^\circ$C, and $T_{to} =$
$T_i \pm \Delta T/2$, at -20 and +50 $^\circ$C. For $T_i = T_{to} = 15$ $^\circ$C, Figure 9, curve C, gives
$\phi \approx 4^\circ$. For $\phi = 4^\circ$, the T_{to} positions define the θ-angle as $\theta = 35.285^\circ$. From
Figure 11, $\phi \approx 4^\circ$, $c_o = 103.5 \times 10^{-12}$, and, from Eq. (19), we obtain $\Delta F_{min} =$
$0.5 c_o (70)^3 = 17.8 \times 10^{-6}$.

23

Figure 11. Second and Third Order Temperature
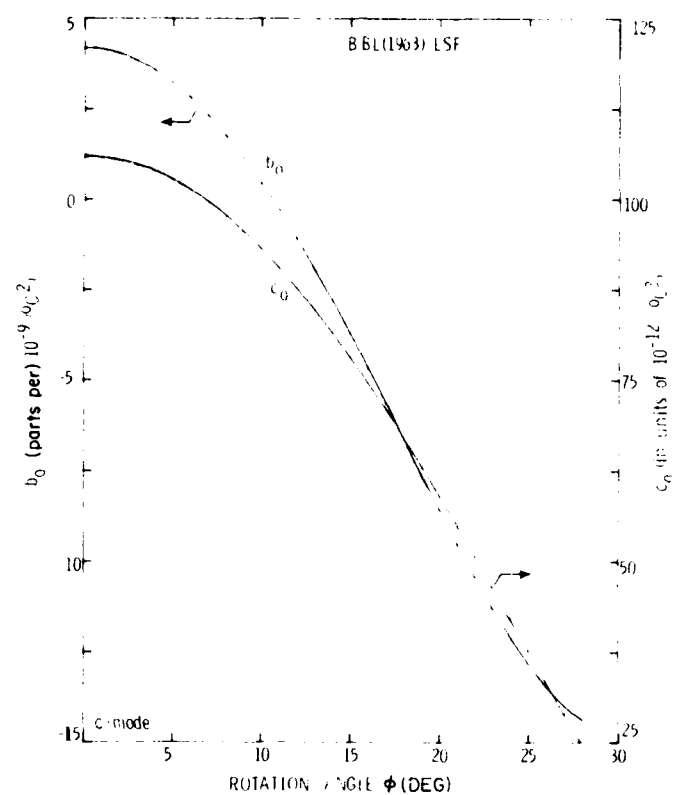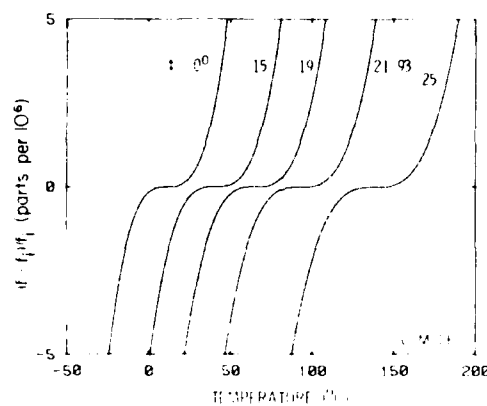Coefficients of Frequency of the c-mode at $T_i = T_{to}$ as a Function of Rotation Angle ϕ

Figure 12. Frequency Offsets as a Function of Temperature for $T_i = T_{to}$ and Selected ϕ-angles Normalized to the Respective Inflection Temperatures

24
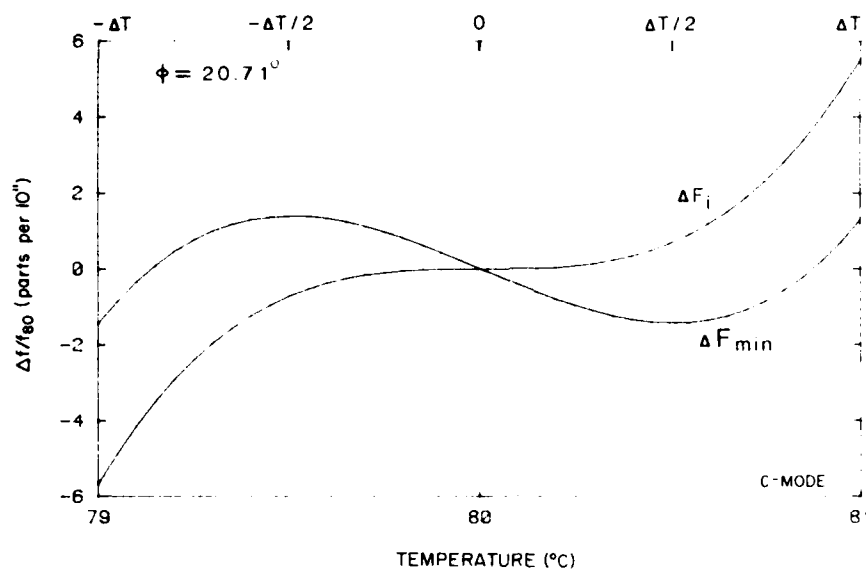
Figure 13. Normalized Frequency Offsets as a Function of Temperature for $\phi = 20.71^{\circ}$. The curve depicted as ΔF_i corresponds to $T_i = T_{to} = 80\,^{\circ}C$. The curve designated as ΔF_{min} is the minimum obtainable frequency offset between 79 and $81\,^{\circ}C$

6. LOCI OF TURNOVER TEMPERATURES

In previous sections we have discussed the special situations arising from $a_o = 0$ and $a_i = 0$. For high precision oscillator applications, the resonator is enclosed in an oven and operated at T_{to}, designed to be several degrees above the highest anticipated environmental temperature. For military applications, T_{to} range between 60 and 100 $^{\circ}C$. The static f(T) characteristic for a specified T_{to} is determined by all $f_n(\phi, \theta)$ coefficients, and a judicious selection of a doubly rotated angular orientation may result in improved performance, regardless of the conditions defined by $a_o = 0$ or $a_i = 0$.

Figure 14 shows (ϕ, θ) loci of T_{to} for c-mode vibrations between 0 and 160 $^{\circ}C$ for selected ϕ-angles between 0 and 26°. These curves are reproduced from Reference 10. For each ϕ-angle the curves are continuous and multivalued. The horizontal markers on the curves indicate $T_i = T_{to}$ values, that is, the lower θ-angle limits for which T_{to} exist. The curve segments above the markers define the upper T_{to}, whereas the curve segments below the markers denote the lower turnover temperatures. $T_i = T_{to}$ increases with ϕ and for a specified T_{to}

10. Kahan, A. (1982) Turnover temperatures for doubly rotated quartz, 36th Annual Symposium on Frequency Control, 170-180.

Figure 14. Turnover Temperatures for the c-mode as a
Function of Rotation Angle θ for Selected ϕ-angles Be-
tween 0 and 26°. The horizontal bars indicate $T_i = T_{to}$
Positions

one may be situated either at the upper or at the lower T_{to}. For a given ϕ, the
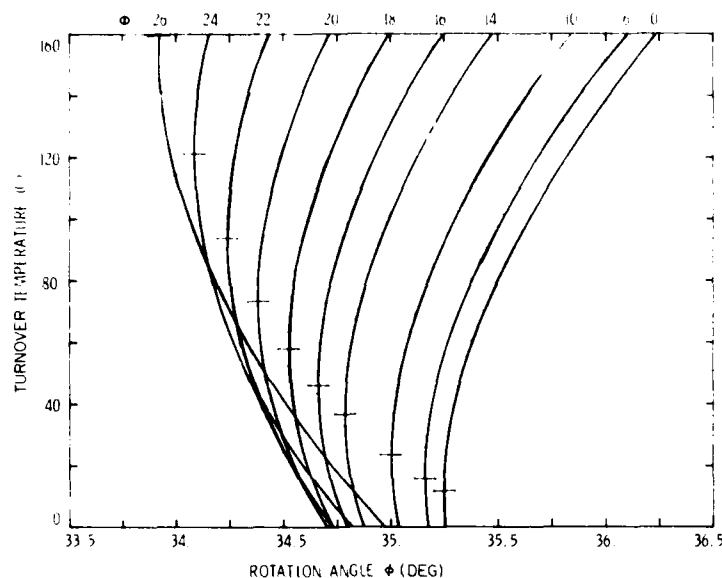slope indicates θ-angle sensitivity, and the figure shows that at $T_i = T_{to}$, small
θ-angle misorientations will drastically shift T_{to}. For $\phi = 0^\circ$, the standard
AT-cut, the most sensitive region is at 12 $^\circ$C, whereas for $\phi = 20^\circ$, the sensi-
tive region has shifted to 73 $^\circ$C. For the SC-cut, $\phi = 21.93^\circ$, a $\Delta\theta = 28''$ mis-
orientation will shift T_{to} from 80 $^\circ$C to 75 $^\circ$C.

Figure 15 shows the same type of information, T_{to} as a function of ϕ, for
selected θ in the -100 to +200 $^\circ$C range. For a given θ, T_{to} is not necessarily
a continuous function. For example, for $\theta = 35.5^\circ$, the upper and lower T_{to}
branches are separated, and for specific ϕ-angles there are defined temperature
ranges where T_{to} do not exist. A clearer illustration may be obtained by pre-
senting this data as (ϕ, θ) loci for constant T_{to}. Figure 16 shows the loci for
T_{to} between 60 and 100 $^\circ$C, in 10 $^\circ$C intervals. Consistent with the fact that
$T_i = T_{to}$ shifts to higher temperatures, T_{to} curves are well separated in θ for
small ϕ-angles, coalesce in the $\phi = 15^\circ$ to $\phi = 25^\circ$ region, and again separate
between $\phi = 25^\circ$ and $\phi = 45^\circ$. For a specific T_{to}, θ decreases with increasing
ϕ up to $\phi \approx 25^\circ$, increases between $\phi \approx 25^\circ$ and $\phi \approx 37^\circ$, and again decreases
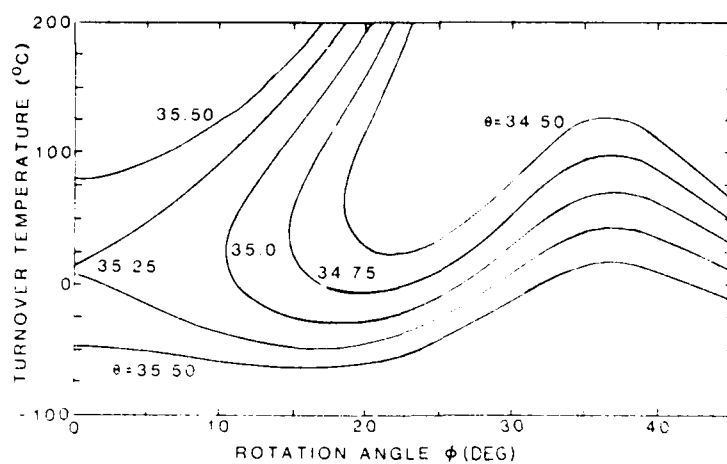with increasing ϕ. We note that a continuous (ϕ, θ) region exists that gives T_{to}

26

Figure 15. Turnover Temperatures for the c-mode as a
Function of Rotation Angle φ for Selected θ-angles Be-
tween 34. 5 and 35. 5°
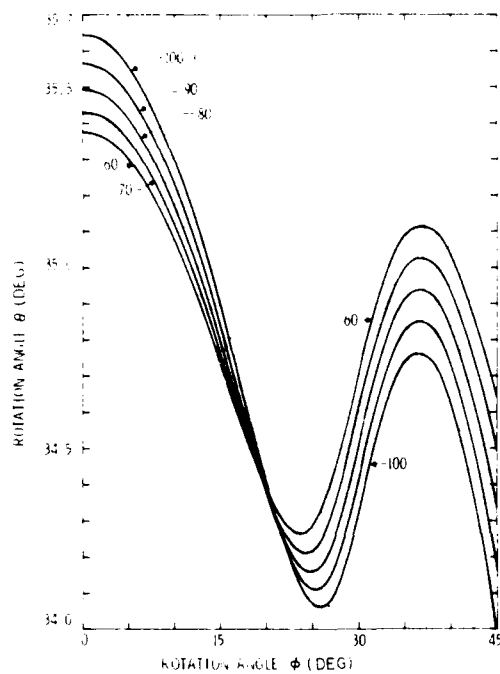
Figure 16. Loci in φ and θ of Constant
Turnover Temperatures Between 60
and 100 °C

27

values between 60 and 100 $^\circ$C. This allows us the flexibility to select an orienta-tion that also optimizes the resonator with respect to some other performance parameter.

The shapes of the curves illustrated in Figure 16 for (ϕ, θ) loci of T_{to} are not peculiar to BBL(1963) LSF. Computations based on BBL(1962) or Adams et al result in similar shapes. Figure 17 shows the (ϕ, θ) loci for c-mode T_{to} = 80 $^\circ$C based on the three $T_n(c_{pq})$ sets. The actual θ-angles differ, but the general pattern is the same. Similar to $T_i = T_{to}$, the higher ϕ-angles serve as sensitive indicators to determine the validity of the various $T_n(c_{pq})$ sets. In this report we are interested in illustrating f(T) behavior, and we omit the T_{to} computations for the angular region between $\phi = 45^\circ$ and $\phi = 60^\circ$, shown in Reference 10. The results for this angular region are very complicated, are influenced by the b- and c-mode crossover near $\phi \approx 50^\circ$, and are very sensitive to $T_n(c_{pq})$. In principle, this would be the ideal angular region from which to derive an accurate set of elastic constants and their temperature coefficients. Similarly, in the $T_i = T_{to}$ and $a_o = 0$ computations we do not show results for $\phi > 30^\circ$. This is because calculated temperatures for these ϕ-angles exceed

Figure 17. Loci in ϕ and θ of 80 $^\circ$C Turnover Temperatures Based on Various Sets of Tem-perature Coefficients of Elastic Constants

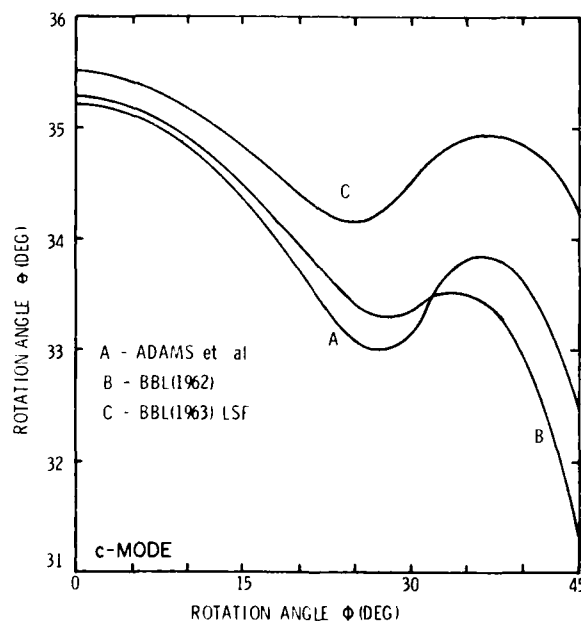200 ^{O}C, the experimental limit of the data from which $T_n(c_{pq})$ were derived. Also, the results are complicated by interferences of the AK-cut and other branches.[10]

7. FREQUENCY OFFSETS FOR T_{to} = 80 ^{O}C

We extend the discussions of the previous sections by considering the static f(T) characteristics at T_{to} = 80 ^{O}C. Figure 18 shows the normalized frequency offsets as a function of temperature for several ϕ-angles for T_{to} = 80 ^{O}C. We note that with increasing ϕ the slope at T_{to} becomes less concave, reflecting the fact that T_i increases with ϕ. At $\phi = 20^O$, on the scale plotted on this figure, the curve at 80 ^{O}C is "flat". For larger ϕ-angles, T_i increases above 80 ^{O}C, T_{to} becomes the lower turnover, and the curves become convex. Figure 19 shows, on an expanded scale, the normalized frequency offsets between 79 and 81 ^{O}C for T_{to} = 80 ^{O}C for selected ϕ-angles. The frequency offsets are normalized to the respective frequencies at 80 ^{O}C. The temperature dependence of frequency decreases with increasing ϕ, and, between $\phi = 20^O$ and $\phi = 22^O$ the curves change from concave to convex. This would imply that there is a unique ϕ for which the frequency offset between 79 and 81 ^{O}C is zero. As illustrated on an expanded scale in Figure 20, this does not happen. The $T_i = T_{to} = 80^{O}$C condition occurs at $\phi = 20.71^O$. For smaller angles, T_{to} = 80°C is satisfied by
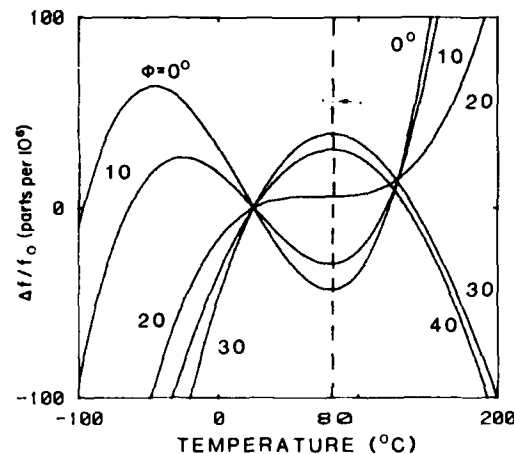
Figure 18. Normalized Frequency Offsets as a Function of Temperature for Selected ϕ-angles and 80 ^{O}C Turnover Temperatures

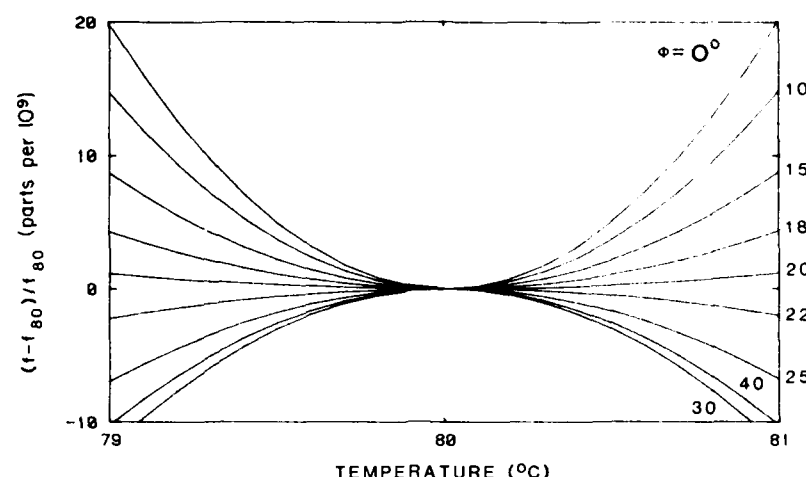Figure 19. Frequency Offsets as a Function of Temperature for Selected ϕ-angles and 80 $^\circ$C Turnover Temperatures. Offsets normalized to respective frequencies at 80 $^\circ$C
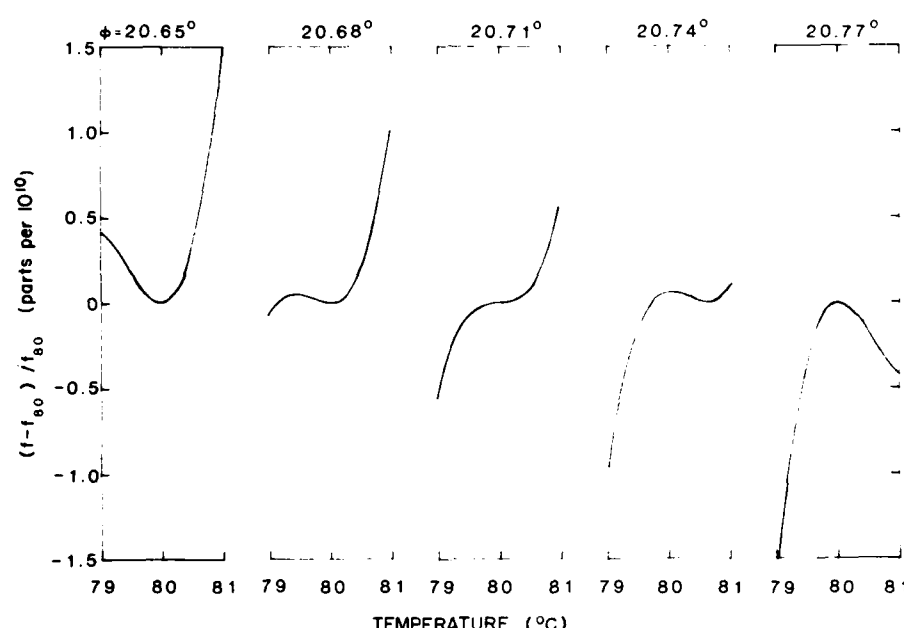

Figure 20. Frequency Offsets as a Function of Temperature for $T_{to} = 80$ $^\circ$C, Normalized to Respective Frequencies at 80 $^\circ$C. $\phi = 20.71^\circ$ corresponds to $T_i = T_{to} = 80$ $^\circ$C

the upper T_{to}. As the ϕ-angle approaches 20.71^{o}, the lower T_{to} (convex) also approaches $80\ ^{o}C$, and the temperature separation between the upper and lower T_{to} decreases. At $\phi = 20.68^{o}$, the two turnover temperatures are within $0.5\ ^{o}C$ of each other, and at 20.71^{o}, the T_{to} coalesce with T_i. (The $\phi = 20.71^{o}$ curve is identical with the ΔF_i curve of Figure 13.) For larger ϕ-values, the T_{to} exchange roles, and $T_{to} = 80\ ^{o}C$ is now given by the convex lower T_{to}. Consequently, with one of the T_{to} values restricted to $80\ ^{o}C$ the frequency offset between 79 and $81\ ^{o}C$ is finite, occurs at $\phi = 20.71^{o}$, and has a value of 1.12×10^{-10}. In Figure 13, the curve marked ΔF_{min}, depicts f(T) corresponding to the minimum frequency offset, with T_{to} not restricted to $80\ ^{o}C$.

Doubly rotated cuts allow improvements in the static f(T) characteristics of the resonator. Figure 21 shows the minimum frequency offsets obtained between 79 and $81\ ^{o}C$ as a function of ϕ, with the turnover temperatures not necessarily restricted to $T_{to} = 80\ ^{o}C$. Figure 22 expands the region between $\phi = 19.4^{o}$ and $\phi = 22.0^{o}$. At $\phi = 0^{o}$ the frequency offset is 20×10^{-9}, decreases at $\phi = 20.71^{o}$ to a minimum of 2.85×10^{-11}, increases at $\phi = 30^{o}$ to 12×10^{-9}, and between $\phi = 30^{o}$ and $\phi = 45^{o}$ it oscillates between 10 and 12×10^{-9}. The top scale of Figure 22 gives $D\phi$, the ϕ-angle referenced to $\phi = 20.71^{o}$.

We have shown that for a resonator operating between 79 and $81\ ^{o}C$, the normalized frequency offset for doubly rotated orientations can be reduced by almost 3 orders of magnitude over the singly rotated cut. This decrease in
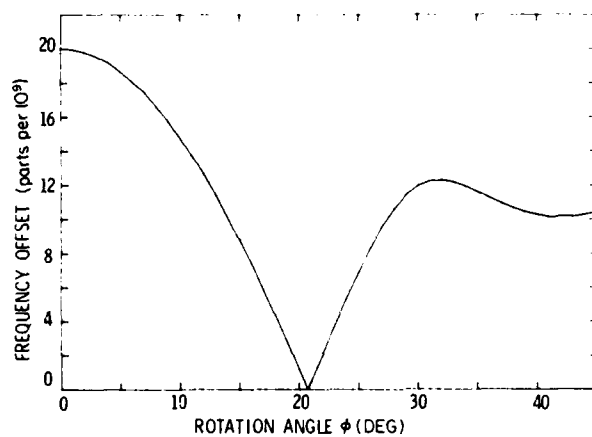

Figure 21. Minimum Frequency Offsets Between 79 and $81\ ^{o}C$ as a Function of Rotation Angle ϕ. Turnover temperature is not necessarily at $80\ ^{o}C$. The θ value is chosen to give minimum offset at each ϕ
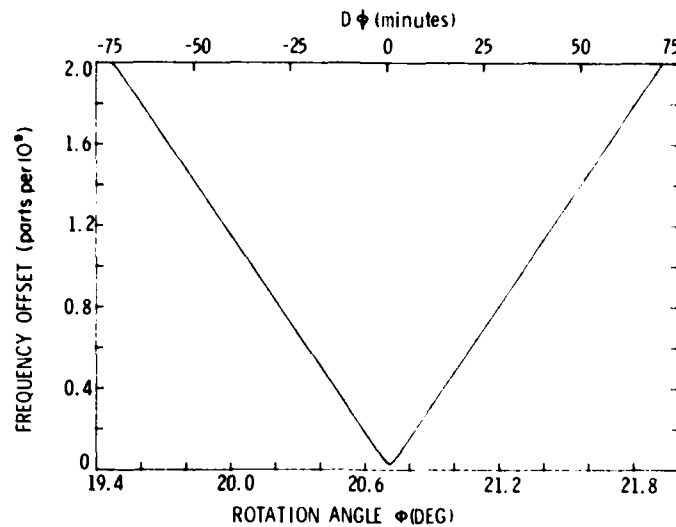
31

Figure 22. Minimum Frequency Offset Between
79 and 81 $^{\circ}$C for ϕ Between 19.4 and 22°. Top
scale references ϕ-angle to ϕ = 20.71°, the an-
gular position of the minimum

temperature sensitivity is at the expense of a decrease in allowable crystal-
lographic tolerances on (ϕ, θ) throughout the resonator fabrication process.
Numerically, the following example illustrates the problem of crystallographic
tolerances. Assume that for the doubly rotated cut operating between 79 and
81 $^{\circ}$C we are satisfied to improve resonator performance by 1 order of magni-
tude over the singly rotated AT-cut, a reduction from $|20 \times 10^{-9}|$ to $|2 \times 10^{-9}|$.
Figure 22 showed that this offset can be satisfied in the continuous angular region
between ϕ = 19.47° and ϕ = 21.93°, a range of 2.46°. We carried out computa-
tions to determine the corresponding θ-angle range, and the tolerances on ϕ or θ
which have to be maintained to achieve this improvement.

Figure 23 shows, for selected ϕ-angles, examples of $|2 \times 10^{-9}|$ frequency
offsets between 79 and 81 $^{\circ}$C. For each ϕ-angle, we also include the curves
defining the minimum offset. For example, for ϕ = 21.0°, the minimum offset
is 0.48×10^{-9}, and the T_{to} are at 79.94 and 85.82 $^{\circ}$C. The two curves with
$|2 \times 10^{-9}|$ offsets have T_{to} at 81.29 and 84.47 $^{\circ}$C, and at 79.05 and 86.73 $^{\circ}$C,
respectively. For all three curves T_i = 82.89 $^{\circ}$C. This is also true for all
other sets as well, that is, T_i is the same for the set, is determined by the
ϕ-angle, and the $|2 \times 10^{-9}|$ limits are obtained by changing the θ-angle.

Figure 24 shows the allowable Dϕ and Dθ deviations and $\pm\Delta\phi$ and $\pm\Delta\theta$ toler-
ances, referenced to ϕ = 20.71°, that have to be maintained to be within $|2 \times 10^{-9}|$
frequency offset in the 79 to 81 $^{\circ}$C range. We reference angular deviations to the
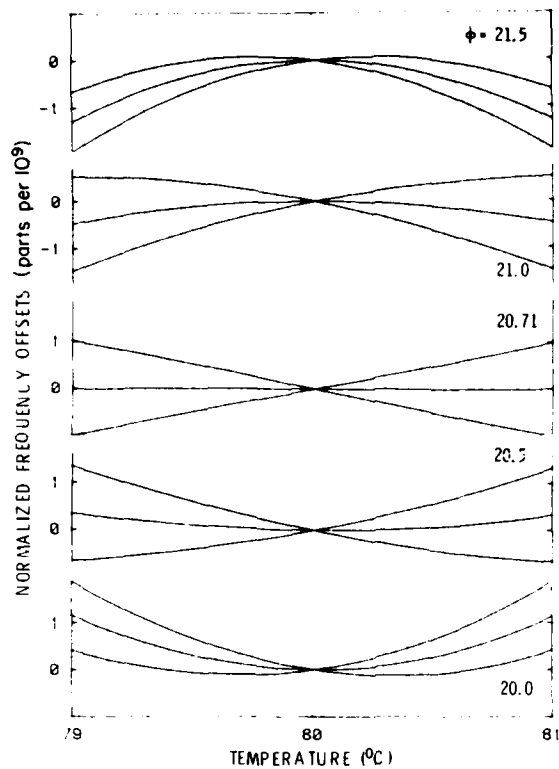
Figure 23. Normalized Frequency Offsets
Between 79 and 81 $^{\circ}$C as a Function of Tem-
perature for Selected ϕ-angles. For each
ϕ-angle, one curve corresponds to the min-
imum, and the other two curves depict the
$|2 \times 10^{-9}|$ offsets

angles corresponding to the absolute minimum frequency offset, that is, (ϕ_o, θ_o) =
$(20.71^{\circ}, 34.33295^{\circ})$. Figure 24(a) gives the $(D\phi, D\theta)$ combinations for the mini-
mum frequency offset curve of Figure 22. It shows that to achieve the minimum
frequency offset attainable at that particular ϕ-angle, each minute of arc mis-
orientation in ϕ must be compensated by $\approx 4.3''$ of arc in θ. If the frequency off-
set is allowed to increase from the local minimum to $|2 \times 10^{-9}|$, the line of
Figure 24(a) becomes an envelope, with $\pm\Delta\phi$ and $\pm\Delta\theta$ tolerances on each $D\phi$ and
$D\theta$ deviation from (ϕ_o, θ_o). These tolerances are plotted in Figures 24(b) and
24(c). For (ϕ_o, θ_o), the corrected angles become $\phi = \phi_o \pm \Delta\phi = \phi_o \pm 15.2''$ and
$\theta = \theta_o \pm \Delta\theta = \theta_o \pm 1.09''$. This points out the sensitivity differences in the ϕ and
θ-angles. The θ-angle is approximately 14 times more sensitive to crystal-
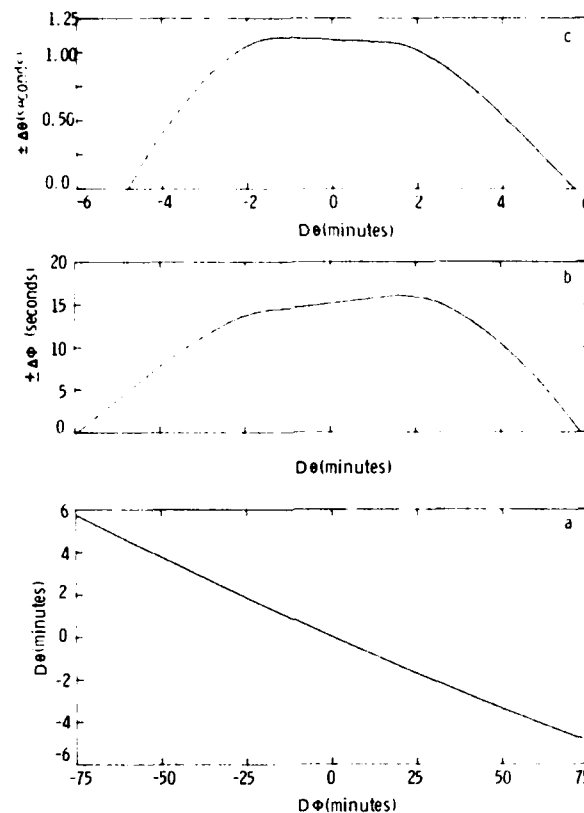lographic misorientations than the corresponding ϕ-angle.

33

Figure 24. Interaction Between ϕ and θ Misorientations. (a) $D\theta$ adjustment for $D\phi$ misorientation for minimum frequency offsets between 79 and 81 $^\circ$C, (b) $\pm\Delta\phi$ tolerance on $D\phi$ misorientation for $|2 \times 10^{-9}|$ frequency offset, and (c) $\pm\Delta\theta$ tolerance on $D\theta$ adjustment for $|2 \times 10^{-9}|$ frequency offset

We illustrate the application of Figure 24 by several additional examples. Assume that the crystal was intended to be oriented to (ϕ_o, θ_o) but measuring it one finds that the θ-angle is misoriented by $D\theta = 3.18'$. The frequency offset corresponding to the misoriented angle is 3.51×10^{-7}. To bring the crystal within the desired frequency offset limit, one can reorient either the ϕ- or the θ-angle. From the relative ϕ and θ sensitivities it seems reasonable that one will always try to reorient the ϕ-angle. Figure 24(a) shows that the ϕ-angle adjustment for the optimum frequency offset is $D\phi = -42.6'$ ($\phi = 20.0^\circ$). Figure 22 showed that the combination ($\phi_o + D\phi$, $\theta_o + D\theta$) = ($\phi_o - 42.6'$, $\theta_o + 3.18'$) gives a frequency deviation of 1.15×10^{-9}. For $D\phi = -42.6'$, Figure 24b gives $\pm\Delta\phi = 9.90''$ as the tolerance that has to be maintained to be within $|2 \times 10^{-9}|$.

Consequently, the corrected ϕ-angle, $\phi = \phi_o + (D\phi \pm \Delta\phi)$, for an angular mis-orientation of $D\theta = 3.18'$ that still maintains $< |2 \times 10^{-9}|$ frequency offset between 79 and 81 ^oC, is $\phi = \phi_o - 42.6' \pm 9.90''$.

Consider another example. One orients the crystal and finds that the ϕ-angle is misoriented by $D\phi = 17.4'$ ($\phi = 21.0^o$). For extraneous reasons it is decided that it is more convenient to accept the misoriented ϕ-angle and optimize the design and adjust the θ-angle. Figure 24(a) shows that the corresponding θ-angle adjustment is $D\theta = -1.23'$. Figure 22 showed that the minimum frequency offset for the adjusted angles is 0.48×10^{-9}. For the given $D\theta$ value, Figure 24(c) gives the tolerance, $\pm\Delta\theta = 1.1''$, which must be maintained to be within $|2 \times 10^{-9}|$. Consequently, the corrected θ-angle, $\theta = \theta_o + (D\theta \pm \Delta\theta)$, for a $D\phi = 17.4'$ mis-orientation that still is within $|2 \times 10^{-9}|$ frequency offset between 79 and 81 ^oC, is $\theta = \theta_o - 1.23' \pm 1.1''$. Incidentally, the maximum allowable tolerances do not occur at $\phi = 20.71^o$, the position of the absolute minimum frequency offset. They are located near $\phi \approx 21.0^o$, the position when one T_{to} is near 79 ^oC and the other one near 81 ^oC.

The static $f(T)$ characteristics for $T_{to} = 80 ^oC$ define $\phi = 20.71^o$ as the optimum doubly rotated orientation. The frequency difference between $T_{to} \pm 1 ^oC$ is not the only criterion to be considered for selecting doubly rotated cuts. The frequency separation between the b- and c-mode of vibrations, and the magnitude of the electromechanical coupling factors, are also important parameters. Figure 25 shows these parameters for $T_{to} = 80 ^oC$. We note that the b- to c-mode frequency separation decreases from 12.6 percent at $\phi = 0^o$ to 9.5 percent at 20.71^o. At the same time the c-mode electromechanical coupling factor decreases from 8.7 percent at $\phi = 0^o$ to 5.4 percent at 20.71^o, whereas the b-mode coupling factor increases from 0 percent to 4.4 percent. Consequently, the improved frequency-temperature characteristics that can be obtained from crystallographically doubly rotated cuts are at the expense of tighter angular tolerances in the fabrication process, a relatively weaker c-mode, and a more complicated oscillator circuit to suppress or isolate the nearby b-mode.
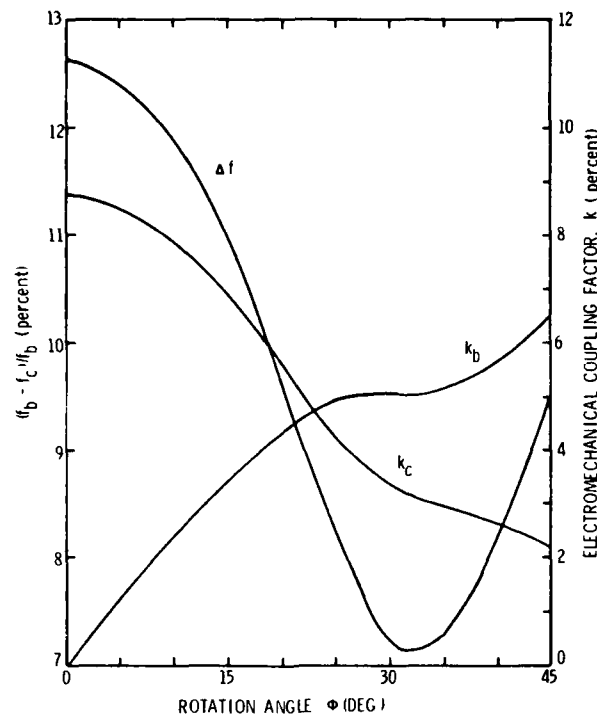
Figure 25. Separation Between b- and c-mode Frequencies (Left Scale), and Electromechanical Coupling Factors (Right-hand Scale) as a Function of Rotation Angle ϕ for 80 °C Turnover Temperatures

8. THE SC-CUT

The advantages and developments of the SC-cut have been reviewed by many investigators.[11-14] Specifically the SC-cut yields improvements in stress insensitivity and compensation of thermal transients. The static f(T) of the SC-cut

11. Kusters, J.A., and Adams, C.A. (1980) Production statistics of SC (or TTC) crystals, 34th Annual Symposium on Frequency Control, 167-174.

12. Kusters, J.A. (1981) The SC-cut - An overview, 1981 Ultrasonics Symposium, (IEEE 81CH1689.9), 402-409.

13. Vig, J.R., Filler, R.L., and Kosinski, J.A. (1982) SC-cut resonators for the temperature compensated oscillators, 36th Annual Symposium on Frequency Control, 181-186.

14. Warner, A.W., Goldfrank, B., and Tsaclas, J. (1982) Further developments in SC cut crystal resonator technology, 36th Annual Symposium on Frequency Control, 208-214.

is no better than other optimally designed doubly rotated cuts. For our purposes it can be defined as the cut oriented at $\varphi = 21.93^{\circ}$. Its behavior is very similar to the description we gave for $\varphi = 20.71^{\circ}$, the optimal angle for operating at $80\,^{\circ}C$.

For the SC-cut, the optimum reference angles corresponding to the absolute minimum frequency offset are calculated as $(\varphi_o, \theta_o)_{sc} = (21.93, 34.24463)^{\circ}$. At these angles $T_i = T_{to} = 92.92\,^{\circ}C$. Figures 8 and 9 show that at $\varphi = 21.93^{\circ}$, BBL(1962) based computations give $\theta = 33.6712^{\circ}$ and $T_i = T_{to} = 102.92$, and Adams et al based coefficients yield $\theta = 33.3941^{\circ}$, and $T_i = T_{to} = 113.96\,^{\circ}C$. Based on BBL(1963) LSF, the optimum operating temperature for the SC-cut is $\approx 93\,^{\circ}C$. The frequency offset for a range of $\Delta T = \pm 1\,^{\circ}C$ around $T_{to} = T_i$ is $\Delta F_i = 1.02 \times 10^{-10}$, whereas the minimum frequency offset that can be obtained in the $\pm 1\,^{\circ}C$ range around $92.92\,^{\circ}C$ is $\Delta F_{min} = 2.58 \times 10^{-11}$. The angular difference between the ΔF_i and ΔF_{min} curves is $\Delta \theta = 0.043''$, similar to the value for $T_{to} = T_i = 80\,^{\circ}C$. The $a_o = 0$ condition is defined by $(21.93, 34.4934)^{\circ}$, at which angles $T_i = 97.44\,^{\circ}C$, and the T_{to} are at 25 and $169.9\,^{\circ}C$, respectively. The experimental T_{to} sensitivity to small variations in φ and θ around $(21.93, 34.115)^{\circ}$ has been published by Kusters and Adams[11] and is reproduced in Vig et al.[9] We obtain similar curves based on BBL(1963) LSF.

In many applications it is desirable to operate the SC-cut at other than the optimal $93\,^{\circ}C$. The right hand scale of Figure 26 shows the minimum frequency offsets ΔF as a function of operating temperature T_{op}, between 60 and $100\,^{\circ}C$, that can be achieved for $\varphi = 21.93^{\circ}$ and variable θ-angles, and a range of $\Delta T = \pm 1\,^{\circ}C$ around T_{op}. For example, the minimum offset for a SC-cut plate optimized for $T_{op} = 60\,^{\circ}C$ and operating in the temperature range of 59 to $61\,^{\circ}C$ is $\Delta F = 5.2 \times 10^{-9}$. A minimum ΔF of 2.6×10^{-11} is reached at $T_{op} = 92.92\,^{\circ}C$, and increases at $T_{op} = 100\,^{\circ}C$ to $\Delta F = 1.07 \times 10^{-9}$. The left hand scale of Figure 26 shows the correction angle $D\theta$, referenced to $(\theta_o)_{sc}$, that is required to shift the minimum frequency offset from $92.92\,^{\circ}C$ to some other operating temperature. At a particular temperature, the minimum frequency offset occurs when T_{op} coincides with T_{to}. The $D\theta$ curve of this figure corresponds to T_{to} variation with θ, and it shows, for example, that for $D\theta = 200''$ the T_{to} is shifted from 93 to $60\,^{\circ}C$. Consistent with results of Figure 21, we note that the minimum frequency offset of $|2 \times 10^{-9}|$ is reached at $T_{op} = 80\,^{\circ}C$. Consequently, one cannot operate an SC-cut crystal below $80\,^{\circ}C$ and still obtain a frequency offset less than $|2 \times 10^{-9}|$ in the $\pm 1\,^{\circ}C$ range of T_{op}.

Figure 24 showed sensitivity curves $D\varphi \pm \Delta \varphi$ and $D\theta \pm \Delta \theta$ around $\varphi = 20.71^{\circ}$. One can construct the same type of curves, with very similar results, for $\varphi = 21.93^{\circ}$. For example, for $T_{op} = 80\,^{\circ}C$, the θ-angle adjustment is $D\theta = -3.46''$
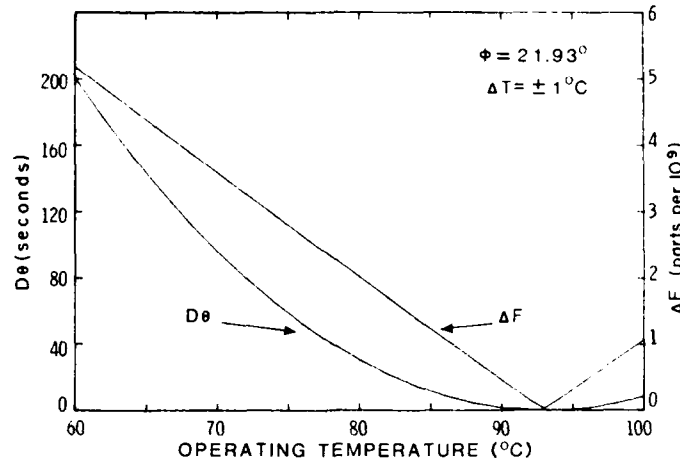
37

Figure 26. Dθ Adjustment as a Function of Operating (Turnover) Temperature for SC-cut, ϕ = 21.93°. Right-hand scale gives the minimum frequency offset in a ±1 °C range around the operating temperature

per minute of Dϕ misorientation. For T_{op} = 80 °C, the minimum frequency offset is not symmetric around ϕ = 21.93°, but follows the curve of Figure 22. For ϕ = 21.93° and Dϕ = -20', the minimum offset is 1.45×10^{-9}, whereas for Dϕ = +20', the offset is 2.54×10^{-9}.

From a practical point of view, ϕ and θ are then selected to give the best compromise for the desired operating temperature, between stress insensitivity, thermal transient response, b- to c-mode separation, electromechanical coupling, static f(T) characteristics, and ease of fabrication.

References

1. Bechmann, R., Ballato, A.D., and Lukaszek, T.J. (1962) Higher-order temperature coefficients of elastic stiffnesses and compliances of α-quartz, Proc. IRE 50:1812-1822.

2. Kahan, A. (1982) Elastic Constants of Quartz, RADC-TR-82-117, AD A121672.

3. Kahan, A. (1982) Temperature Coefficients of the Elastic Constants of Quartz, RADC-TR-82-224, AD A125709.

4. Kusters, J.A., Adams, C.A., Yashida, H., and Leach, J.G. (1977) TTC's - Further developmental results, 31st Annual Symposium on Frequency Control, 3-7.

5. Ballato, A.D. (1977) Doubly rotated thickness mode plate vibrators, Physical Acoustics, Vol. XIII, W.P. Mason and T.N. Thurston, Eds., Academic Press, New York, pp. 115-181.

6. Bechmann, R., Ballato, A.D., and Lukaszek, T.J. (1963) Higher-Order Temperature Coefficients of Elastic Stiffnesses and Compliances of α-Quartz, USAELRDL TR 2261.

7. Adams, C.A., Enslow, G.M., Kusters, J.A., and Ward, R.W. (1970) Selected topics in quartz crystal research, 24th Annual Symposium on Frequency Control, 55-63, AD 746210.

8. Bechmann, R. (1956) Frequency-temperature-angle characteristics of AT-type resonators made of natural and synthetic quartz, Proc. IRE 44:1600-1607.

9. Vig, J., Washington, J.W., and Filler, R.L. (1981) Adjusting the frequency vs. temperature characteristics of SC-cut resonators by contouring, 35th Annual Symposium on Frequency Control, 104-109.

10. Kahan, A. (1982) Turnover temperatures for doubly rotated quartz, 36th Annual Symposium on Frequency Control, 170-180.

11. Kusters, J.A., and Adams, C.A. (1980) Production statistics of SC (or TTC) crystals, 34th Annual Symposium on Frequency Control, 167-174.

12. Kusters, J.A. (1981) The SC-cut - An overview, 1981 Ultrasonics Symposium, (IEEE 81CH1689.9), 402-409.

13. Vig, J.R., Filler, R.L., and Kosinski, J.A. (1982) SC-cut resonators for the temperature compensated oscillators, 36th Annual Symposium on Frequency Control, 181-186.

14. Warner, A.W., Goldfrank, B., and Tsaclas, J. (1982) Further developments in SC cut crystal resonator technology, 36th Annual Symposium on Frequency Control, 208-214.

END

FILMED

8